JOURNAL OF AGRICULTURAL AND FOOD CHEMISTRY

Article

pubs.acs.org/JAFC

The UVA and Aqueous Stability of Flavonoids Is Dependent on B-Ring Substitution

Sabia Maini, Heather L. Hodgson, and Ed S. Krol*

Drug Design and Discovery Research Group, College of Pharmacy and Nutrition, University of Saskatchewan, 110 Science Place, Saskatoon, SK, S7N 5C9, Canada

Supporting Information

ABSTRACT: Flavonols such as kaempferol and quercetin are believed to provide protection against ultraviolet (UV)-induced damage to plants. Recent in vitro studies have examined the ability of flavonols to protect against UV-induced damage to mammalian cells. Stability of flavonols in cell culture media, however, has been problematic, especially for quercetin, one of the most widely studied flavonols. As part of our investigations into the potential for flavonols to protect skin against UV-induced damage, we have determined the stability of a series of flavonols that differ only in the number of substituents on the B-ring. We measured the stability of these flavonols over time to UVA radiation, Dulbecco's modified Eagle's medium (DMEM), and Dulbecco's phosphate-buffered saline (DPBS) using high performance liquid chromatography with UV detection (HPLC−UV). The identification of the breakdown products of flavonols was accomplished by using a hybrid quadrupole linear ion trap mass spectrometer coupled with liquid chromatography. Tandem mass spectrometric analysis (MS/MS) of flavonol photoproducts was confirmed by comparing with the known standard samples. We have determined that flavonol stability decreases with increasing B-ring substitution, suggesting that future investigation of potential photoprotective flavonols will need to be cognizant of this trend.

KEYWORDS: *flavonol, stability, sunscreen, ultraviolet radiation, cell media*

INTRODUCTION

The flavonols are a family of naturally occurring polyphenols that are present in a wide variety of plant species. The synthesis of several of the flavonols such as quercetin and kaempferol are known to be upregulated in a number of plants after exposure to elevated levels of ultraviolet (UV) radiation[1−3] presumably due to their ability to provide protection for plants against UV radiation-induced damage. An increasing number of studies are examining whether naturally occurring flavonols such as kaempferol, quercetin, and myricetin could provide protection against UV radiation-induced damage in humans.[4−9] These flavonols have been shown to affect a variety of signaling pathways associated with UV radiation-induced damage. Kaempferol can inhibit UVB-induced COX-2 expression by suppressing Src kinase activity in JB6 P+ cells.[6] Quercetin has been shown to protect primary human keratinocytes from UV-induced inflammatory cytokine production through the NfκB pathway[4] and protect against UVB-induced skin damage in a hairless mouse model.[10] Quercetin has also demonstrated the ability to spare the sunscreen octyl methoxycinnamate[11] and the anti-inflammatory ketoprofen from UV radiation-induced decomposition.[12] Myricetin regulates UVB-induced MMP-9 expression through the suppression of Raf kinase[13] and PI3 kinase[7] activity in mouse skin, suppression of Fyn kinase activity in JB6 P+ cells and mouse skin,[8] and inhibition of Akt-mediated survival signaling in UVB-induced skin carcinogenesis in HaCaT cells.[14]

Among these flavonols, quercetin is the least expensive, and it has been utilized in the majority of initial studies. It has been observed, however, that quercetin can be unstable in the cell media used in some of these studies. Quercetin can be stabilized by the concurrent use of ascorbic acid[15] although this resulted in a decrease in its proapoptotic effect, which led the authors to suggest that the quercetin breakdown products may be responsible for the proapoptotic effects. Further, if quercetin is not stabilized, it is capable of inducing c-Fos expression in UVB treated HaCaT cells, an important cellular event in the tumor promotion phase.[16] Another study examining chemopreventive effects of quercetin in Caco-2 cells found that ascorbic acid stabilization of quercetin actually led to an increase in oncogenic gene expression.[17]

Quercetin has been shown to be unstable in aqueous solution[18−21] and to visible and UV radiation.[22−27] Although efforts have been directed toward improving quercetin stability including pivaloxymethyl derivatization of the 3-OH group,[28] and incorporation of quercetin in microemulsions,[10,29] nanoparticles,[30] or lipid microparticles,[31] there remain concerns regarding the potential deleterious properties of unstabilized quercetin.

The question of the stability of all of the major flavonols (kaempferol, quercetin, and myricetin) under study as photoprotectants needs to be addressed. Olson[16] claims that myricetin has the potential to be a superior protectant based on the observation that it is stable in cell media compared to quercetin.[8] Myricetin differs from quercetin by having a 3,4,5-trihydroxy substituted B-ring vs quercetin which has a 3,4-dihydroxy substituted B-ring (Figure 1). We found this

Received: December 13, 2011
Revised: June 19, 2012
Accepted: June 20, 2012
Published: June 20, 2012

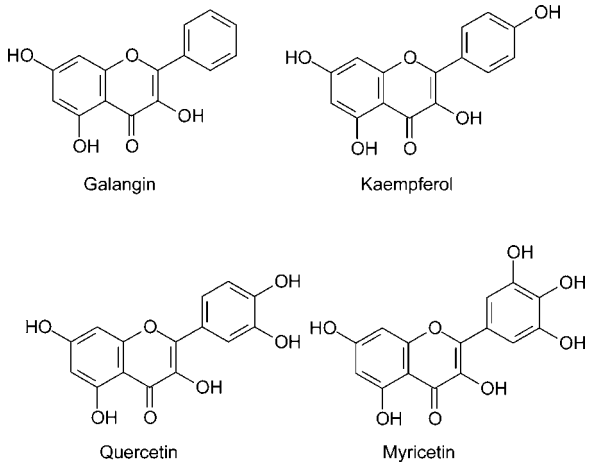

Figure 1. Structure of galangin, kaempferol, quercetin, and myricetin.

observation of greater myricetin stability to be puzzling as previous indications in the literature suggested that the oxidative stability of flavonoids decreases as the number of hydroxyl groups on the B-ring increases.[32,33] Most of these studies, however, investigated mixtures of flavonoids (catechins, flavonols, flavanones), making direct comparison of the flavonols difficult.[32,34]

We have previously shown that both UVA and UVB radiation cause quercetin to decompose to three major products, two of which appear to be the result of a direct photolytic reaction.[22] We hypothesize that B-ring substitution of the flavonols galangin, kaempferol, quercetin, and myricetin (Figure 1) influences their stability in aqueous solution and to UV radiation. Our study has two primary goals, to determine the relative stability of the flavonols in DMEM and DPBS and to determine if the same relative stability is observed after exposure to UVA radiation in methanol.

MATERIALS AND METHODS

1. General. Quercetin dihydrate ($C_{15}H_{10}O_7 \cdot 2H_2O$, M_w = 338.26), myricetin ($C_{15}H_{10}O_8$, M_w = 318.235), kaempferol ($C_{15}H_{10}O_6$, M_w = 286.23), galangin ($C_{15}H_{10}O_5$, M_w = 270.24), 2,4,6-trihydroxybenzoic acid, benzoic acid, 2,4,6-trihydroxybenzaldehyde, 3,4-dihydroxybenzoic acid, and 1,3,5-trihydroxybenzene were purchased from Sigma (St. Louis, MO). Dulbecco's modified Eagle's medium (DMEM) was purchased from ATCC (Burlington, ON). Dulbecco's phosphate-buffered saline (DPBS) was purchased from Gibco Invitrogen (Burlington, ON). LC/MS grade water and methanol was purchased from Fisher Scientific Canada (Ottawa, ON). Water was purified using a Millipore Super Q water system with one carbon cartridge followed by two ion exchange cartridges (Bedford, MA).

UVA irradiations were carried using two F20T12/BL/HO UVA lamps (National Biological Corp., Beachwood, OH) filtered to remove UVC with an intensity of 740 $\mu W \cdot cm^{-2}$ at 365 nm as measured with a UVP UVX-36 sensor.

2. High Performance Liquid Chromatography–Ultraviolet Photodiode Array (HPLC–UV-PDA). HPLC–UV-PDA analysis was performed on an Alliance system using a Waters 2996 photodiode array detector. Aliquots of 100 μL were taken from solutions containing flavonols treated with either UVA, DMEM, or DPBS and injected directly onto a 250 × 4.6 mm Allsphere ODS-2 column, 5 μm particle size (Alltech, Calgary, AB, Canada). Data was processed using Empower software (Waters, Milford, MA). Elution was carried out in gradient mode using two components: A = 0.1% formic acid in water, B = 0.1% formic acid in methanol.

For quercetin analysis the gradient was as follows: 0 to 10 min, linear gradient from 90% A to 40% A; 10 to 25 min, isocratic 40% A; 25 to 28 min, linear gradient from 40% A to 90% A; 28 to 30 min, isocratic 90% A.

For myricetin, kaempferol, and galangin analysis the mobile phase was the same and the gradient was 20 min, linear gradient from 70% A to 10% A; 20 to 25 min, isocratic 10% A; 25 to 28 min, linear gradient from 10% A to 70% A; 28 to 30 min, isocratic 70% A. Flow rate was 1.2 mL/min.

3. HPLC–MS/MS analysis. High performance liquid chromatography–tandem mass spectrometry (HPLC–MS/MS) analysis was carried out at room temperature on an AB SCIEX 4000 QTRAP (AB SCIEX instruments) quadrupole linear ion trap mass spectrometer coupled to an Agilent 1100 system consisting of an Agilent 1100 G1311A pump and an Agilent 1100 G1329A autosampler (Agilent Technologies, Mississauga, ON). Analyst 1.5.1 software from AB SCIEX was used for controlling the equipment and for data acquisition.

Separation of flavonols and their photoproducts in methanol was achieved using an Allsphere ODS-2 3 μm column (2.1 mm by

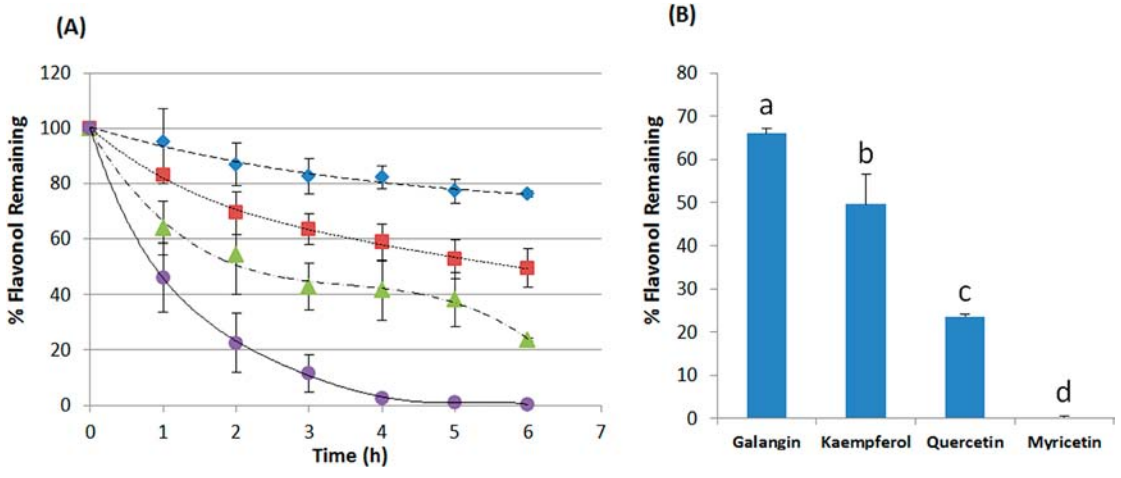

Figure 2. (A) Time course for loss of flavonol in methanol (50 μM) exposed to UVA radiation (740 $\mu W \cdot cm^{-2}$, 365 nm). Individual time points are the peak areas from HPLC chromatograms (flavonol λ_{max}). Results are shown as % flavonol remaining as determined by HPLC peak area. Error bars represent standard deviation from the mean of three replicates. ◆ = galangin (358 nm), ■ = kaempferol (365 nm), ▲ = quercetin (368 nm), ● = myricetin (374 nm). (B) The bar graph represents the mean levels of % flavonol remaining (±SD) after 6 h in UVA. These results are the mean of three independently performed experiments, and statistically significant differences ($p < 0.05$) between groups are indicated by labels containing different letters.

dx.doi.org/10.1021/jf3016128 | J. Agric. Food Chem. 2012, 60, 6966–6976

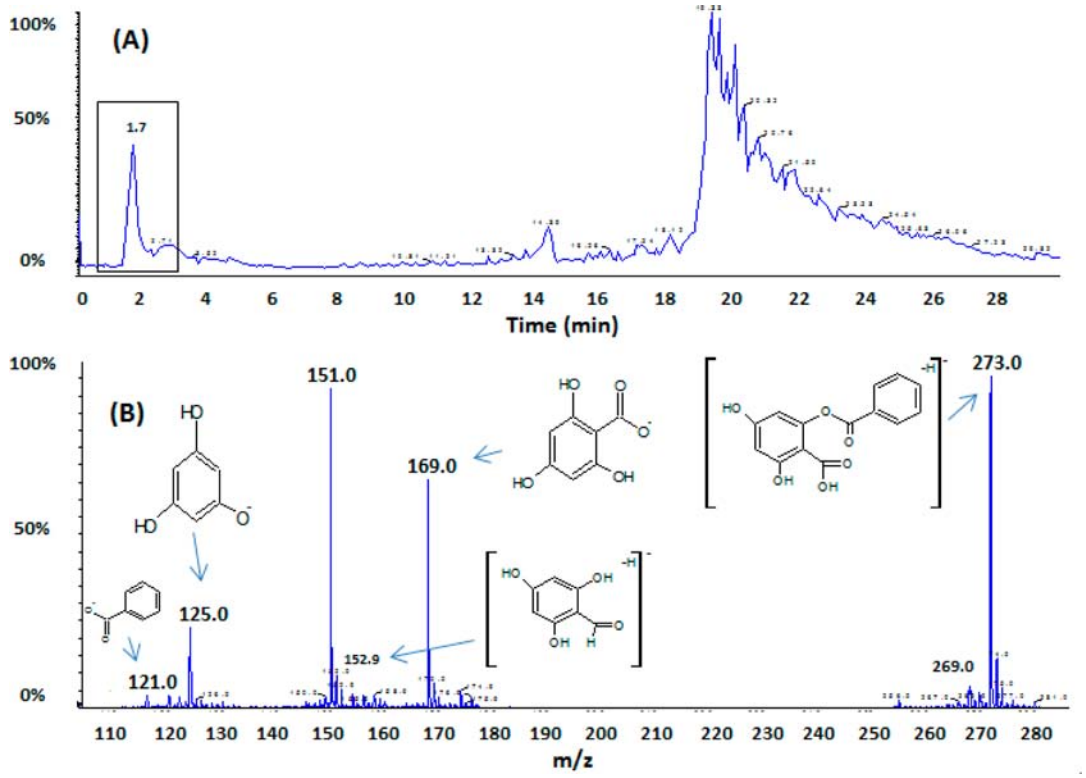

Figure 3. (A) Negative-ion mode HPLC−ESI-MS total ion chromatogram of galangin in methanol (50 μM) with excess of benzophenone exposed to UVA radiation (740 μW·cm^{-2}, 365 nm) for 6 h. (B) HPLC−ESI-MS spectrum from 1.1 to 2.6 min showing the major decomposition products of galangin after exposure to UVA radiation.

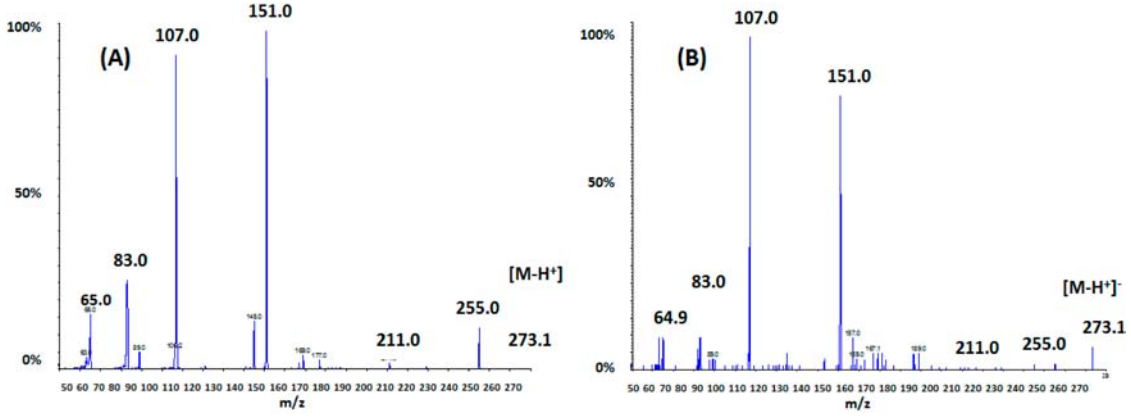

Figure 4. (A) Enhanced product ion (HPLC−MS/MS) spectrum of the $[M - H]^-$ precursor ion m/z 273 corresponding to depside of galangin (50 μM) in methanol with excess of benzophenone exposed to UVA radiation. (B) Enhanced product ion (HPLC−MS/MS) spectrum of the $[M - H]^-$ precursor ion m/z 273 corresponding to depside of galangin (0.25 mM) in DMEM incubated at room temperature for 12 h.

150 mm) with the same gradient of water and methanol with 0.1% formic acid described above at a flow rate of 200 μL/min. A similar gradient of water and methanol with 0.1% formic acid was used for identification of flavonols and their breakdown products in DMEM, but with the flow rate at 150 μL/min for first 5 min, in order to decrease the ion suppression effect of DMEM. The injection volume for flavonols in methanol and DMEM reaction was at 15 μL. In between runs, a blank sample (100% methanol) was injected to avoid any sample carryover.

The mass spectrometer was operated in negative ionization mode using electrospray ionization (ESI). The ion spray voltage was set to −4500 V, the curtain gas was 10 psi, ion source gas (1) was set at 10 psi, and ion source gas (2) was 40 psi. The source temperature was set at 200 °C.

Tandem mass spectrometric analysis on the breakdown products of flavonols were performed using enhanced product ion (EPI) scans. Collision activated dissociation (CAD) was performed by using nitrogen gas for tandem analysis, and the collision energy (CE) was optimized ranging from −20 eV to −35 eV.

4. UV Irradiation. Myricetin, kaempferol, quercetin, and galangin solutions were prepared in methanol (final concentration 50 μM) and placed in quartz cells. The quartz cells were exposed to UVA radiation with an intensity of 700 μW·cm^{-2} for 6 h. The samples (100 μL) were collected hourly from 0 to 6 h and analyzed by direct injection onto the HPLC−UV-PDA. The photostability study of the flavonols was performed by comparing the relative amount of flavonol remaining after UVA exposure by measuring peak area at the λ_{max} for each flavonol.

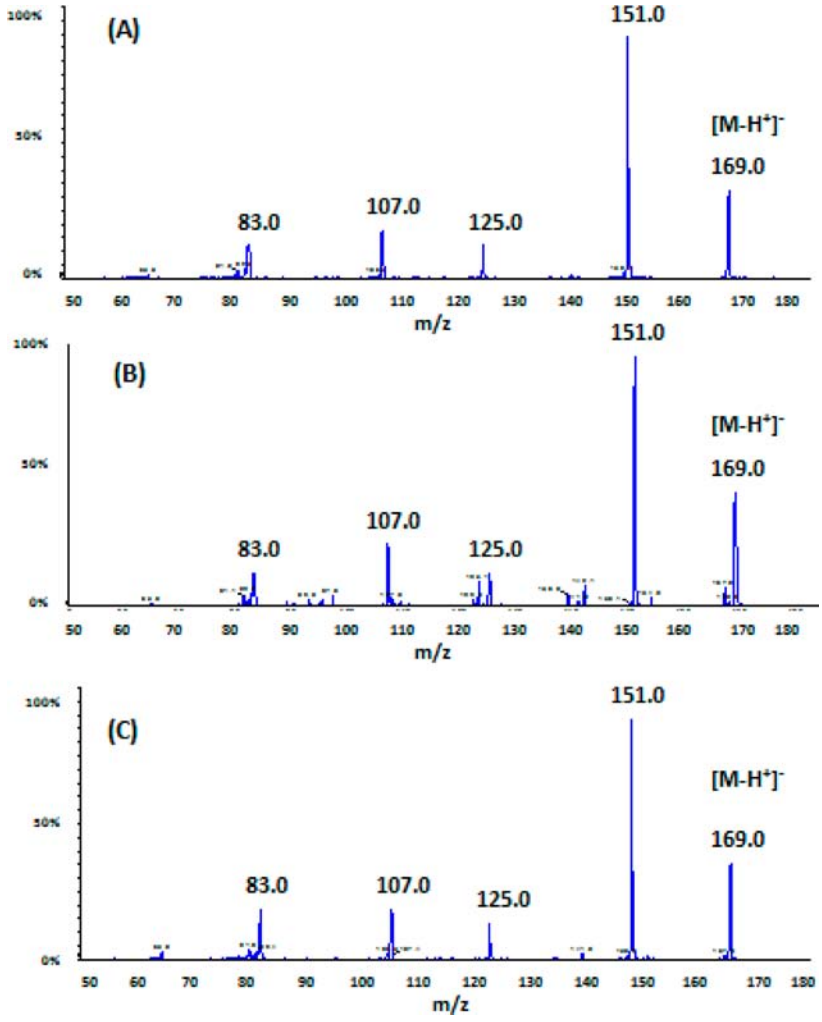

Figure 5. Enhanced product ion (HPLC−MS/MS) spectrum of the $[M - H]^-$ precursor ion m/z 169 from (A) galangin in methanol with benzophenone exposed to UVA radiation; (B) galangin in DMEM; and (C) corresponding pure standard sample of 2,4,6-trihydroxybenzoic acid.

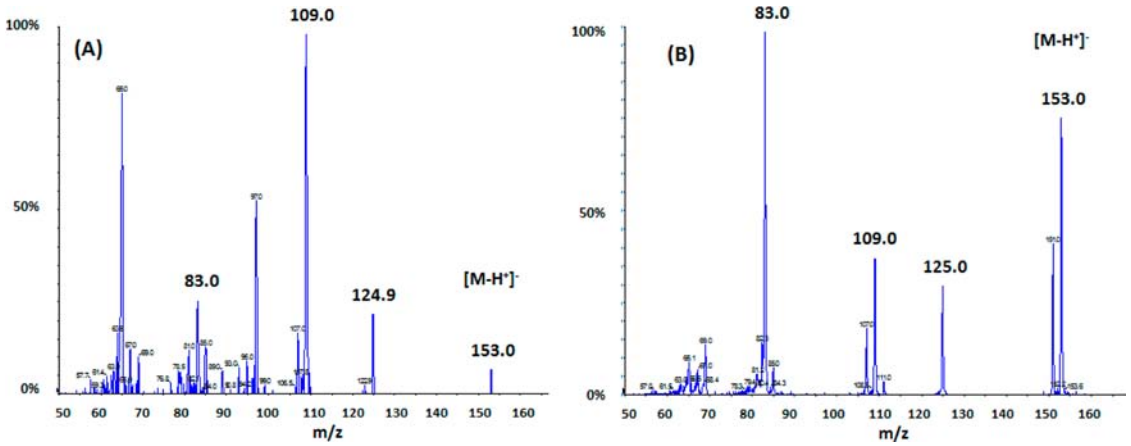

Figure 6. Enhanced product ion (MS/MS) spectrum of the $[M - H]^-$ precursor ion m/z 153 from (A) galangin in methanol with benzophenone exposed to UVA radiation and (B) its corresponding pure standard sample of 2,4,6-trihydroxybenzaldehyde.

Analysis of UVA radiation-induced breakdown products of flavonols was performed by using HPLC−ESI-MS/MS. 50 μM solutions of each flavonol in methanol with an excess of benzophenone was exposed to UVA radiation for different exposure times. Galangin and kaempferol being comparatively more stable were exposed to UVA radiation for 6 h, compared to quercetin and myricetin, for which the exposure time was reduced to 90 min. Separation and identification of flavonol breakdown products was achieved by direct injection of samples onto the HPLC−mass spectrometer.

5. Stability of Flavonols in Dulbecco's Modified Eagle's Medium (DMEM) or Dulbecco's Phosphate-Buffered Saline (DPBS). DMEM or DPBS was placed in a tissue culture dish and maintained at room temperature (22 ± 1 °C). 1 mM stock solutions of myricetin, kaempferol, quercetin, and galangin were added to the

dx.doi.org/10.1021/jf3016128 | J. Agric. Food Chem. 2012, 60, 6966−6976

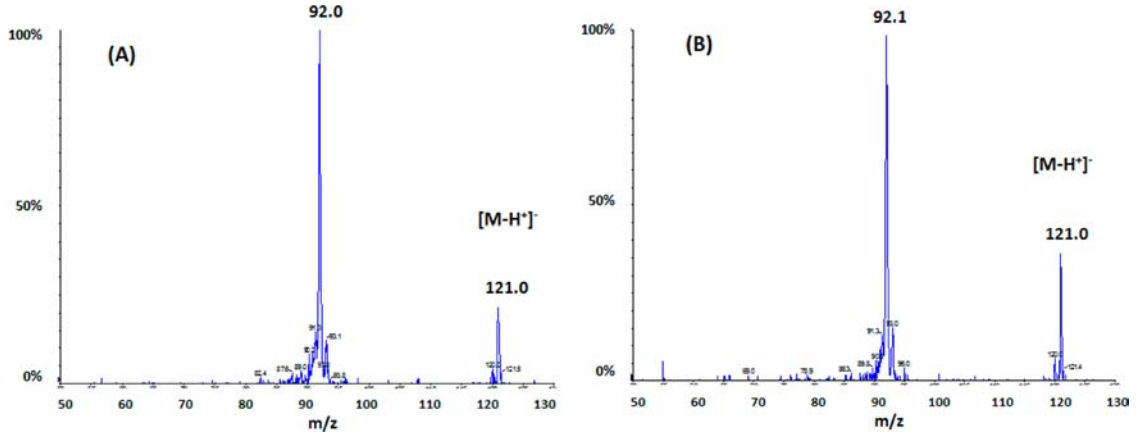

Figure 7. Enhanced product ion (MS/MS) spectrum of the $[M - H]^-$ precursor ion m/z 121 from (A) galangin in methanol with benzophenone exposed to UVA radiation and (B) its corresponding pure standard sample of benzoic acid.

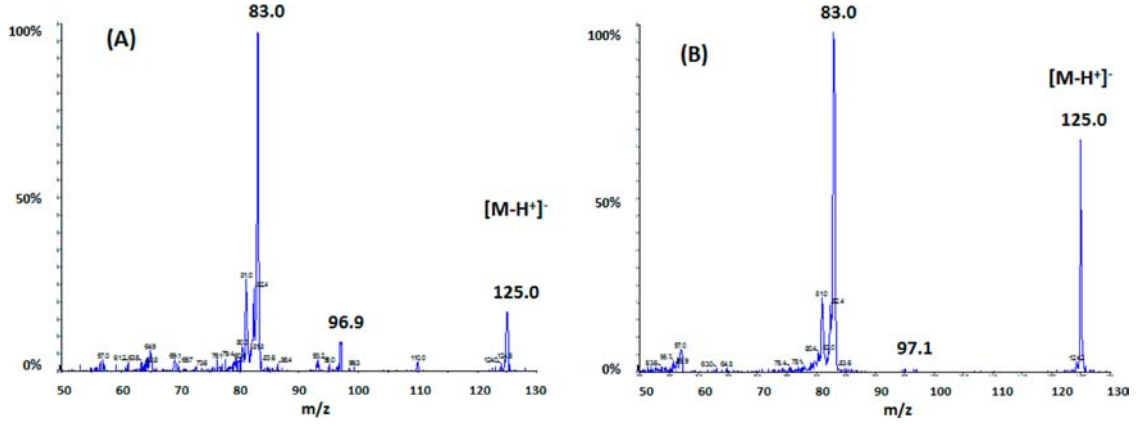

Figure 8. Enhanced product ion (MS/MS) spectrum of the $[M - H]^-$ precursor ion m/z 125 from (A) galangin in methanol with benzophenone exposed to UVA radiation and (B) its corresponding pure standard sample of 1,3,5-trihydroxybenzene.

DMEM or DPBS to a final flavonol concentration of 50 μM. Aliquots of 100 μL were taken hourly from 0 to 6 h and analyzed immediately by HPLC–UV-PDA. The time-course samples were compared to the DMEM or DPBS 0 h time point to determine the amount of flavonol remaining by measuring peak area at the λ_{max} for each flavonol.

HPLC–MS/MS analysis on the stability of flavonols in DMEM included sample preparation by overnight incubation of 0.25 mM flavonols in DMEM. The samples were dried and reconstituted in 100% methanol, followed by filtration. The identification of flavonols and their breakdown products in DMEM was accomplished by tandem mass spectrometry coupled to liquid chromatography as indicated above.

6. Statistics. Significant differences in % remaining flavonol were assessed with one-way analysis of variance with Tukey's test for pairwise multiple comparisons using SPSS software (IBM SPSS statistics version 19, Markham, ON, Canada). The level of significance was set at $P < 0.05$.

RESULTS AND DISCUSSION

We are currently investigating the ability of naturally occurring flavonols to act as topical skin photoprotectants. The stability of these flavonols is an important consideration as there have been numerous reports about the instability of flavonols in different experimental conditions. Our studies were designed to determine if B-ring substitution could be correlated with flavonol stability in aqueous systems and to UVA radiation. The decision to study DMEM is the result of its frequent use as a medium for cell culture studies involving flavonols. For all of the stability studies, we tested the four flavonols at room temperature (22 ± 1 °C) for 6 h. We used HPLC with different detection methods to determine the amount of flavonol remaining in solution (HPLC–UV-PDA) or to identify the flavonol breakdown products (HPLC–ESI-MS/MS with enhanced resolution and in product ion mode).

Stability of Flavonols to UVA Radiation. Since photoprotection studies being carried out on flavonols frequently involve exposure of the flavonols to UV radiation, we decided to determine the stability of the flavonols to UVA radiation. We chose to use UVA as all of the flavonols under study have a strong absorbance in the UVA (galangin, 358 nm; kaempferol, 365 nm; quercetin, 368 nm; myricetin, 374 nm) and previous studies on quercetin UV stability in our lab determined that both UVA and UVB caused quercetin decomposition.[22]

Figure 2A shows the time-course results for the loss of starting material as % remaining flavonol. After 1 h galangin levels were significantly different from quercetin and myricetin levels ($p < 0.05$) and kaempferol was significantly different from myricetin ($p < 0.05$). Notably, after 6 h, all of the flavonol levels were significantly different from each other (Figure 2B) ($p < 0.05$). None of the flavonols decomposed completely over the time course. Galangin was the most stable over 6 h (76% remaining) and myricetin the least stable over 6 h (<1% remaining). The general pattern of flavonol stability (galangin > kaempferol > quercetin > myricetin) demonstrated that the number of B-ring hydroxyl groups is inversely related to flavonol UVA stability over a 6 h time course.

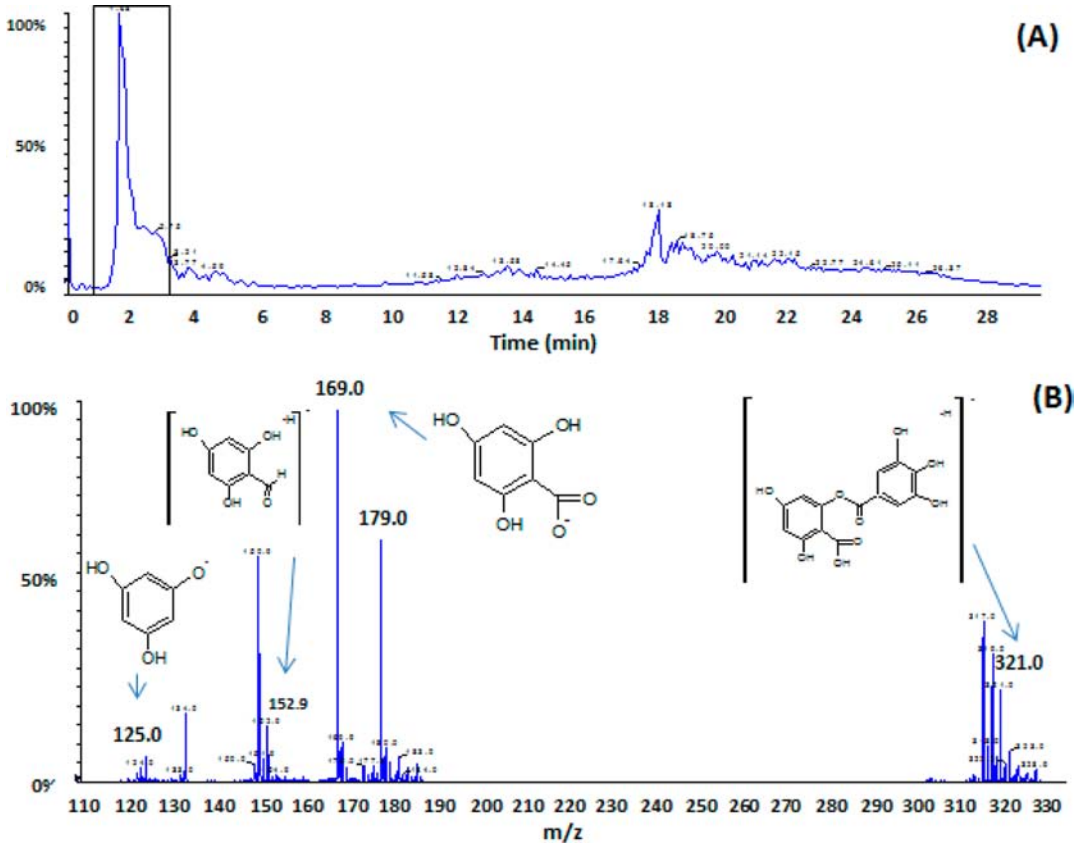

Figure 9. (A) Negative-ion mode HPLC−ESI-MS total ion chromatogram of myricetin in methanol (50 μM) with excess of benzophenone exposed to UVA radiation (740 μW·cm^{-2}, 365 nm) for 90 min. (B) HPLC−ESI-MS spectrum from 0.8 to 3.6 min showing most distinctive photoproducts of myricetin after exposure to UVA radiation.

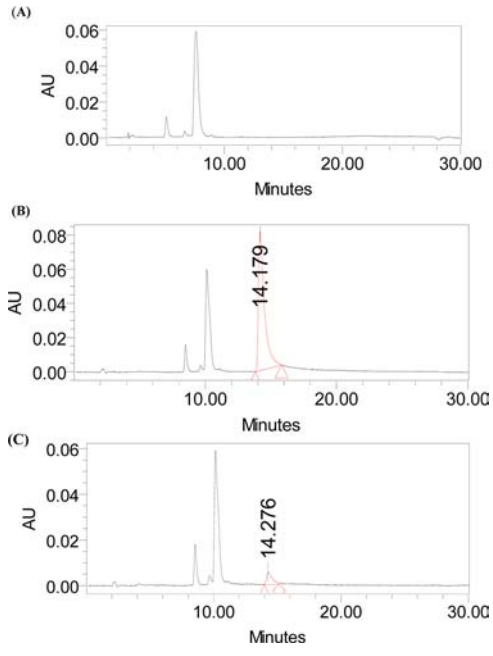

Figure 10. (A) HPLC−UV (368 nm) chromatogram of DMEM. (B) HPLC−UV (368 nm) chromatogram of quercetin (50 μM, 14.17 min) in DMEM at 0 h. (C) HPLC−UV (368 nm) chromatogram of quercetin (50 μM, 14.27 min) in DMEM at 3 h.

We had previously shown that UVA exposed quercetin decomposes to three products and wanted to confirm that all of the flavonols tested followed the same UV decomposition pathway.[22] In order to increase the amount of product formed, we repeated our UVA experiments with the most stable (galangin) and least stable (myricetin) flavonols in which the photosensitizer benzophenone was added. We had previously observed that no changes in quercetin UV decomposition products were observed when benzophenone was used.[22]

We confirmed that the major decomposition products of UVA irradiated flavonols are the depside, its major decomposition product 2,4,6-trihydroxybenzoic acid, and the 2,4,6-trihydroxybenzaldehyde photoproduct. The total ion chromatogram and negative ion ESI spectrum of an early eluting peak for UVA treated galangin are shown in Figures 3A and 3B respectively. The ESI spectrum in Figure 3B is consistent with the presence of the depside (m/z 273, $[M - H^+]^-$), the depside decomposition products 2,4,6-trihydroxybenzoic acid (m/z 169, $[M - H^+]^-$), benzoic acid (m/z 121, $[M - H^+]^-$), and 1,3,5-trihydroxybenzene (m/z 125, $[M - H^+]^-$), and the photoproduct 2,4,6-trihydroxybenzaldehyde (m/z 153, $[M - H^+]^-$). Some galangin (m/z 269, $[M - H^+]^-$) also appears in the spectrum. Figures 4−8 illustrate the results from the enhanced product ion spectra for the galangin decomposition products (Figure 4A, depside (m/z 273); Figure 5A, 2,4,6-trihydroxybenzoic acid (m/z 169); Figure 6A, 2,4,6-trihydroxybenzaldehyde (m/z 153); Figure 7A, benzoic acid (m/z 121); Figure 8A, 1,3,5-trihydroxybenzene (m/z 125)). The enhanced product ion spectra for the standards of 2,4,6-trihydroxybenzoic acid (m/z 169), 2,4,6-trihydroxybenzaldehyde (m/z 153), benzoic acid (m/z 121), and 1,3,5-trihydroxybenzene (m/z 125) are shown in Figures 5C, 6B, 7B, and 8B respectively. The total ion

dx.doi.org/10.1021/jf3016128 | J. Agric. Food Chem. 2012, 60, 6966−6976

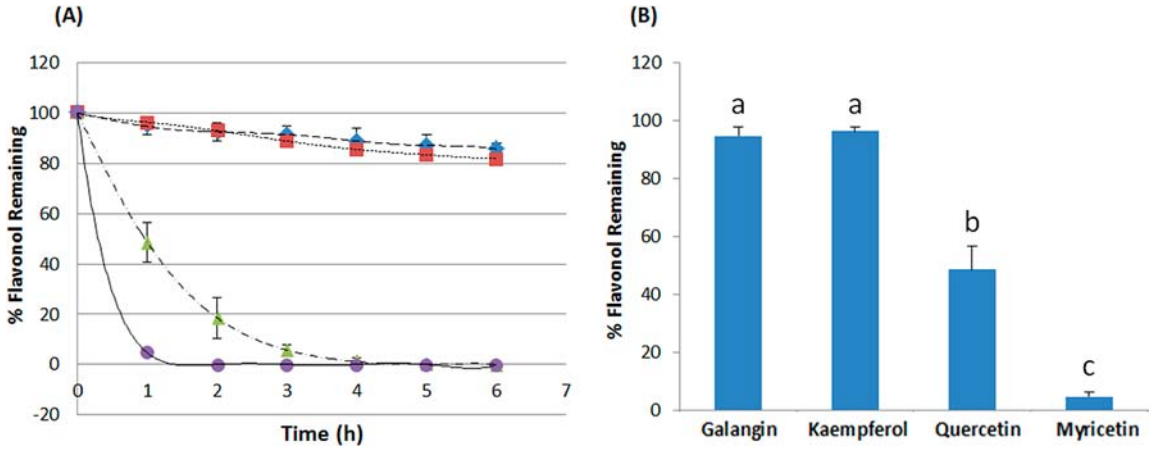

Figure 11. (A) Time course for loss of flavonol in DMEM (50 μM) at 25 °C. Individual time points are the peak areas from HPLC chromatograms (flavonol λ_{max}). Results are shown as % flavonol remaining as determined by HPLC peak area. Error bars represent standard deviation from the mean of three replicates. ◆ = galangin (358 nm), ■ = kaempferol (364 nm), ▲ = quercetin, (368 nm), ● = myricetin (373 nm). (B) The bars represent the mean levels of % flavonol remaining (±SD) after 1 h in DMEM at 25 °C. These results are the mean of three independently performed experiments, and statistically significant differences ($p < 0.05$) between groups are indicated by labels containing different letters. The results containing labels with the same letters are not significantly different.

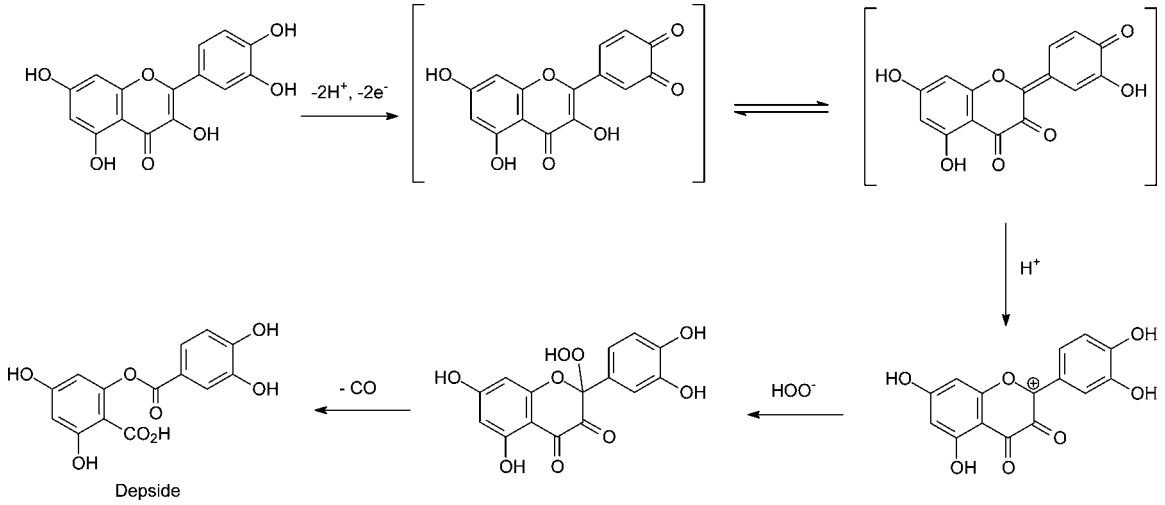

Figure 12. Proposed reaction mechanism for quercetin oxidation, adapted from ref 35.

chromatogram for myricetin is shown in Figure 9A, and the negative ESI spectrum for myricetin is shown in Figure 9B, with the corresponding depside (m/z 321, $[M - H^+]^-$), and the decomposition products 2,4,6-trihydroxybenzoic acid (m/z 169, $[M - H^+]^-$) and 1,3,5-trihydroxybenzene (m/z 125, $[M - H^+]^-$), and the photoproduct 2,4,6-trihydroxybenzaldehyde (m/z 153, $[M - H^+]^-$). Unfortunately we were unable to confirm the presence of the 3,4,5-trihydroxybenzoic acid which shares an identical mass to the 2,4,6-trihydroxybenzoic acid.

Stability of Flavonols in DMEM. In our HPLC−UV-PDA experiments the flavonols separated from background components present in DMEM (Figure 10A). We could not, however, clearly observe the flavonol decomposition products with this technique as they appear to coelute with the background components of DMEM as shown for quercetin (14.17 min) in Figures 10B and 10C. The other flavonols displayed similar retention times (galangin, 18 min; kaempferol, 15 min; myricetin, 11.24 min). Confirmation of the decomposition products required HPLC−ESI-MS/MS, which is described below. Figure 11A shows the time-course results for the loss of starting material as % remaining flavonol. After 3 h the loss of both myricetin and quercetin exceeded 90% by HPLC−UV-PDA. Conversely more than 80% of kaempferol and galangin remained after 6 h in DMEM. After both 1 and 6 h, galangin and kaempferol levels were significantly different from quercetin and myricetin levels ($p < 0.05$). In addition, at 1 h quercetin and myricetin levels were significantly different from each other (Figure 11B) ($P < 0.05$). The general pattern of flavonol stability (galangin > kaempferol ≫ quercetin > myricetin) was in agreement with our observations for UVA stability that the flavonols with the fewest B-ring hydroxyl groups (galangin and kaempferol) are the most stable in DMEM over a 6 h time course and the flavonols with the greatest degree of B-ring substitution (quercetin and myricetin) are the least stable over the entire 6 h time course.

Krishnamachari[33,35] suggested that the ability of flavonols to form a B-ring *ortho*-quinone facilitates the formation of a critical C-ring carbocation intermediate in the oxidative decomposition of flavonols (Figure 12). Of the flavonols that we examined in this study only myricetin and quercetin can readily form a B-ring *ortho*-quinone, which is in agreement with our observation that these two flavonols decompose more rapidly than

dx.doi.org/10.1021/jf3016128 | J. Agric. Food Chem. 2012, 60, 6966−6976

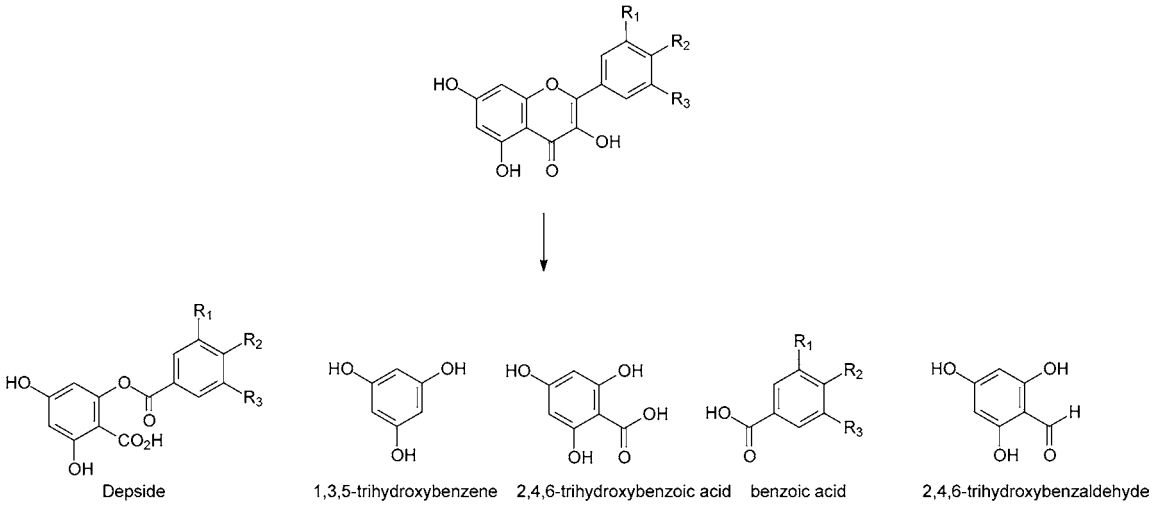

Figure 13. Structures of breakdown products of flavonols investigated after exposure to UVA radiation. Galangin: $R_1 = R_2 = R_3 = H$. Myricetin: $R_1 = R_2 = R_3 = OH$.

kaempferol and galangin. In addition, Brown's σ^+ parameters would infer that the carbocation intermediate in Figure 12 would be stabilized by hydroxyl groups on the B-ring, suggesting that within the group of flavonols the absence of a 4′-OH should result in increased stability of the parent flavonol. Finally, the contributions of the 3′ and 5′ hydroxyl groups in myricetin and quercetin would be expected to stabilize the *para*-quinone methide precursor of the carbocation intermediate, facilitating decomposition via the C-ring carbocation intermediate.[36] Unsubstituted phenols typically do not form *para*-quinone methides readily.

In order to confirm that this decomposition pathway was indeed responsible for the results we had observed, we identified the decomposition products using HPLC–ESI-MS/MS. Standards of the anticipated decomposition products were first analyzed, and then the DMEM treated samples were assessed. The background from DMEM made it difficult to positively identify the flavonol decomposition products. In addition, we found it difficult to separate the anticipated benzoic acid derivatives (Figure 13) as they all eluted close to the solvent front under our chromatographic conditions. In an effort to maximize our product signals we repeated our experiments with the most stable (galangin) and least stable (myricetin) flavonols in which we increased flavonol concentration to 0.25 mM in DMEM for HPLC–ESI-MS/MS analysis.

Sample mass spectral results are shown for the DMEM decomposition products of galangin (Figures 4B, 5B). Similar results were observed for myricetin, which differed from galangin in that it possessed a greater depside mass (m/z 321) and produced no benzoic acid (data not shown). We observed no aldehyde products for the DMEM treated flavonols, which corresponds with our previous results for quercetin in which the aldehyde appears to be a unique photoproduct.[22] The products we observed for our DMEM-mediated flavonol decomposition study suggest to us that the number and location of hydroxyl groups on the B-ring can facilitate decomposition in several ways: by stabilization of a flavonol C-ring carbocation intermediate; by allowing formation of a B-ring *ortho*-quinone intermediate, a likely precursor of the C-ring carbocation; and by stabilization of the *para*-quinone methide, also a presumed C-ring carbocation precursor.[33,35]

Stability of Flavonols in pH 7.2 DPBS. In an effort to determine whether the decomposition of the flavonols in DMEM was a result of aqueous solution pH or other components of DMEM, we carried out the same study using DPBS at the same pH as DMEM. In all cases the flavonols were separated from background components present in DPBS (Figures 14A, 14B). Flavonol decomposition products were not

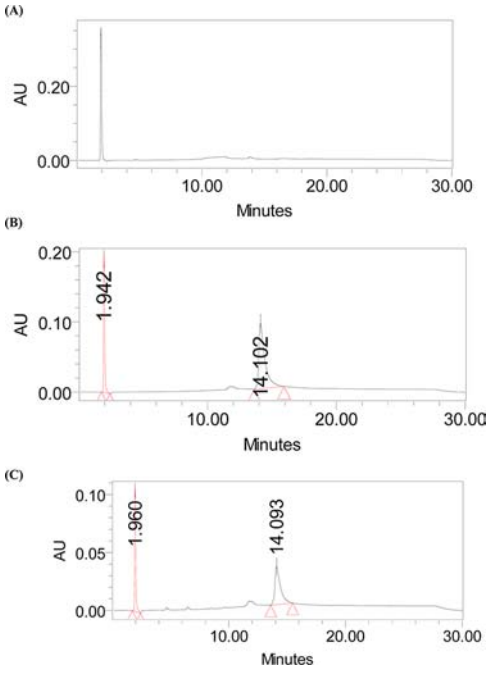

Figure 14. (A) HPLC–UV (254 nm) chromatogram of DPBS. (B) HPLC–UV (254 nm) chromatogram of quercetin (50 μM, 14.10 min) in DPBS at 0 h. (C) HPLC–UV (254 nm) chromatogram of quercetin (50 μM, 14.09 min) in DPBS at 6 h.

clearly observed, however, and again appear to coelute in the DPBS background (Figure 14C); however, ESI-MS/MS studies confirm that the 2,4,6-trihydroxybenzoic acid is the major product. Figure 15A shows the time-course results for the loss of starting material as % remaining flavonol. After a 1 h incubation, galangin was significantly different from kaempferol and quercetin

dx.doi.org/10.1021/jf3016128 | J. Agric. Food Chem. 2012, 60, 6966–6976

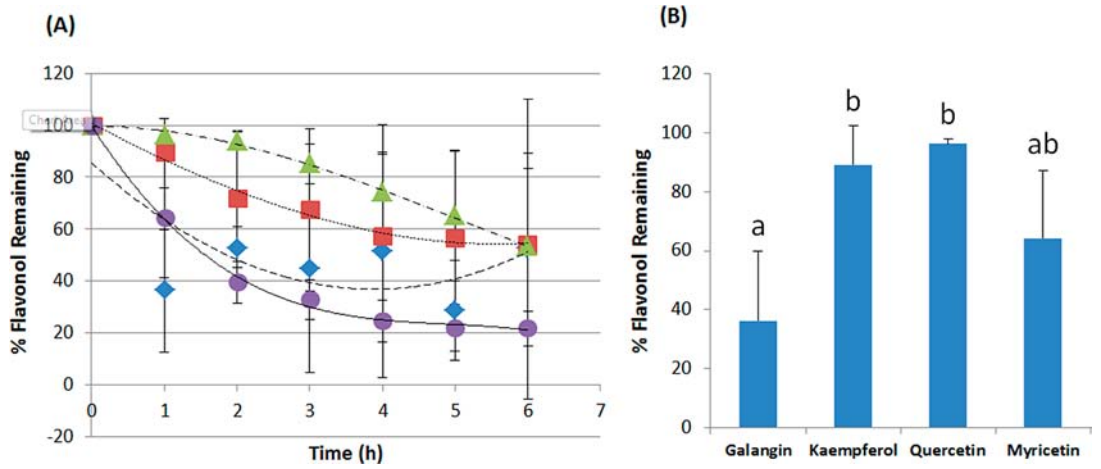

Figure 15. (A) Time course for loss of flavonol in DPBS (50 μM) at 25 °C. Individual time points are the peak areas from HPLC chromatograms (flavonol λ_{max}). Results are shown as % flavonol remaining as determined by HPLC peak area. Error bars represent standard deviation from the mean of three replicates. ◆ = galangin (358 nm), ■ = kaempferol (254 nm), ▲ = quercetin, (254 nm), ● = myricetin (254 nm). (B) The bar graph represents the mean levels of % flavonol remaining (±SD) after 1 h in DPBS at 25 °C. These results are the mean of three independently performed experiments, and statistically significant differences ($p < 0.05$) between groups are indicated by labels containing different letters. The results containing labels with the same letters are not significantly different.

whereas after 6 h incubation there was no significant difference between any of the flavonol levels (Figure 15B) ($P < 0.05$). Notably, 21% of myricetin is still present at 6 h and more than 50% of the other three flavonols remains. Unfortunately the data points for the galangin stability study show a great deal of variability, which likely affected our final result; we are uncertain as to the source of this large variation for galangin. Unlike our results in DMEM, the DPBS study did not demonstrate any clear trend for flavonol stability, rather we observed that after 6 h galangin, kaempferol, and quercetin showed similar levels of product loss (52%, 54%, 53% respectively), with myricetin showing a greater, although not significant, loss (78%).

Fe, Ca, and Mg are present in DMEM but absent in DPBS, and these metals may be sufficient to cause greater oxidation in the DMEM study via chelation to the 3′,4′-B-ring hydroxyl groups which only myricetin and quercetin possess.[37] Others have observed that flavonoids, including quercetin, can generate hydrogen peroxide in cell culture media, with DMEM generating the highest levels[38] and that a flavonoid catechol group was a determining factor in the level of hydrogen peroxide generated in cell culture media.[39] It seems plausible that the production of hydrogen peroxide from an interaction between the catechol moiety and metal ions in solution could enhance the rate of flavonol decomposition in DMEM relative to DPBS. We did not determine whether any metal ions were present in DPBS as our intent was to compare commercially available buffer solutions that are typically utilized in studies on the biological activity of flavonols. The presence of any metal ions in DPBS should, however, be low in comparison to DMEM. The use of buffers which are free of metal ions may minimize the stability issues we have observed with flavonols; however, for the purpose of studies on the biological activity of flavonols, this is not likely practical.

In summary, we determined that flavonol decomposition in DMEM or through UVA radiation, but not in DPBS, is dependent on the number of B-ring hydroxyl groups. We identified the major decomposition products, and they are consistent with the presence of a C-ring carbocation intermediate; the UVA studies also showed the presence of an A-ring benzaldehyde which is consistent with the photoproducts we observed previously in our study of quercetin photodecomposition.[22] In the presence of DMEM the B-ring hydroxyl groups appear to contribute in several ways, including the following: formation of hydrogen peroxide through a catechol−metal interaction; stabilization of a C-ring carbocation intermediate and a B-ring *para*-quinone methide; and allowance of formation of an initial *ortho*-quinone intermediate. Stabilization of the C-ring carbocation and quinone intermediates by the B-ring hydroxyl groups would contribute to the decomposition of the UVA treated flavonols. The presence of the trihydroxybenzoic acid and the absence of any detectable levels of depside in the DPBS experiment suggest that the rate of depside formation is comparable to depside hydrolysis.

Our results suggest that kaempferol and galangin, because of their greater stability to UVA and DMEM, may be attractive alternatives to study as photoprotectants. Although one study has demonstrated that UVA-induced MMP expression in human dermal fibroblasts was improved with increasing flavonol B-ring substitution, this study required incubation for 24 h in media, which likely resulted in decomposition of the flavonols such that the decomposition products may have contributed to inhibition of MMP expression.[40]

Preliminary studies on the photoprotective properties of kaempferol have been carried out,[6] but we could find no evidence of photoprotective studies involving galangin, although it has been studied in various cell lines for anticancer properties. Galangin has been shown to provide a protective effect in LNCaP and DU145 prostate cells through an increase in HIF-1α and HIF-2α levels[41] and by increasing TRAIL-induced apoptosis.[42] Galangin also demonstrated proapoptotic effects in leukemia cells,[43,44] and inhibited ER$^-$ Hs578T cell proliferation via suppression of cyclin D3.[45] Suppression of COX-2 in JT74A.1 macrophages[46] by galangin suggests that it may be promising as a photoprotectant as kaempferol was shown to suppress UVB-induced COX-2 expression.[6]

In conclusion, our studies suggest that flavonol stability increases with decreasing B-ring substitution. As a result future studies on the potential photoprotective properties of the flavonols must pay careful attention to flavonol stability and the biological properties of any flavonol decomposition products.

■ ASSOCIATED CONTENT

Supporting Information

Proposed fragmentation pathways of galangin depside *m/z* 273, 2,4,6-trihydroxybenzoic acid, and 2,4,6-trihydroxybenzaldehyde. This material is available free of charge via the Internet at http://pubs.acs.org.

■ AUTHOR INFORMATION

Corresponding Author

*Phone: 306-966-2011. Fax: 306-966-6377. E-mail: ed.krol@usask.ca.

Funding

E.S.K. is supported by the Natural Sciences and Engineering Research Council (NSERC) and the College of Pharmacy & Nutrition, S.M. is a recipient of a University of Saskatchewan GTA, and H.L.H. is a recipient of a NSERC-USRA.

Notes

The authors declare no competing financial interest.

■ ACKNOWLEDGMENTS

We wish to thank Anas El-Aneed for advice with the mass spectral interpretations and Deb Michel and Joshua Buse for technical assistance.

■ ABBREVIATIONS USED

DMEM, Dulbecco's modified Eagle's medium; FBS, fetal bovine serum; HPLC−UV-PDA, high performance liquid chromatography−ultraviolet photodiode array detection; DPBS, Dulbecco's phosphate-buffered saline; UV, ultraviolet radiation; UVA, ultraviolet radiation A; UVB, ultraviolet radiation B

■ REFERENCES

(1) Wilson, K. E.; Wilson, M. I.; Greenberg, B. M. Identification of the flavonoid glycosides that accumulate in *Brassica napus* L. cv. Topas specifically in response to ultraviolet B radiation. *Photochem. Photobiol.* **1998**, *67*, 547−553.

(2) Wilson, K. E.; Thompson, J. E.; Huner, N. P. A.; Greenberg, B. M. Effects of ultraviolet-A exposure on ultraviolet-B-induced accumulation of specific flavonoids in Brassica napus. *Photochem. Photobiol.* **2001**, *73*, 678−684.

(3) Solovchenko, A.; Schmitz-Eiberger, M. Significance of skin flavonoids for UV-B-protection in apple fruits. *J. Exp. Bot.* **2003**, *54*, 1977−1984.

(4) Vicentini, F. T.; He, T.; Shao, Y.; Fonseca, M. J.; Verri, W. A., Jr.; Fisher, G. J.; Xu, Y. Quercetin inhibits UV irradiation-induced inflammatory cytokine production in primary human keratinocytes by suppressing NF-kappaB pathway. *J. Dermatol. Sci.* **2011**, *61*, 162−168.

(5) Yang, Y. M.; Son, Y. O.; Lee, S. A.; Jeon, Y. M.; Lee, J. C. Quercetin Inhibits alpha-MSH-stimulated Melanogenesis in B16F10 Melanoma Cells. *Phytother. Res.* **2011**, *25*, 1166−1173.

(6) Lee, K. M.; Lee, K. W.; Jung, S. K.; Lee, E. J.; Heo, Y. S.; Bode, A. M.; Lubet, R. A.; Lee, H. J.; Dong, Z. Kaempferol inhibits UVB-induced COX-2 expression by suppressing Src kinase activity. *Biochem. Pharmacol.* **2010**, *80*, 2042−2049.

(7) Jung, S. K.; Lee, K. W.; Byun, S.; Lee, E. J.; Kim, J. E.; Bode, A. M.; Dong, Z.; Lee, H. J. Myricetin inhibits UVB-induced angiogenesis by regulating PI-3 kinase in vivo. *Carcinogenesis* **2010**, *31*, 911−917.

(8) Jung, S. K.; Lee, K. W.; Byun, S.; Kang, N. J.; Lim, S. H.; Heo, Y. S.; Bode, A. M.; Bowden, G. T.; Lee, H. J.; Dong, Z. Myricetin suppresses UVB-induced skin cancer by targeting Fyn. *Cancer Res.* **2008**, *68*, 6021−6029.

(9) Fahlman, B. M.; Krol, E. S. Inhibition of UVA and UVB radiation-induced lipid oxidation by quercetin. *J. Agric. Food Chem.* **2009**, *57*, 5301−5305.

(10) Vicentini, F. T.; Fonseca, Y. M.; Pitol, D. L.; Iyomasa, M. M.; Bentley, M. V.; Fonseca, M. J. Evaluation of protective effect of a water-in-oil microemulsion incorporating quercetin against UVB-induced damage in hairless mice skin. *J. Pharm. Pharm. Sci.* **2010**, *13*, 274−285.

(11) Scalia, S.; Mezzena, M. Photostabilization effect of quercetin on the UV filter combination, butyl methoxydibenzoylmethane-octyl methoxycinnamate. *Photochem. Photobiol.* **2010**, *86*, 273−278.

(12) Nakajima, A.; Tahara, M.; Yoshimura, Y.; Nakazawa, H. Study of compounds suppressing free radical generation from UV-exposed ketoprofen. *Chem. Pharm. Bull. (Tokyo)* **2007**, *55*, 1431−1438.

(13) Jung, S. K.; Lee, K. W.; Kim, H. Y.; Oh, M. H.; Byun, S.; Lim, S. H.; Heo, Y. S.; Kang, N. J.; Bode, A. M.; Dong, Z.; Lee, H. J. Myricetin suppresses UVB-induced wrinkle formation and MMP-9 expression by inhibiting Raf. *Biochem. Pharmacol.* **2010**, *79*, 1455−1461.

(14) Kim, W.; Yang, H. J.; Youn, H.; Yun, Y. J.; Seong, K. M.; Youn, B. Myricetin inhibits Akt survival signaling and induces Bad-mediated apoptosis in a low dose ultraviolet (UV)-B-irradiated HaCaT human immortalized keratinocytes. *J. Radiat. Res.* **2010**, *51*, 285−296.

(15) Olson, E. R.; Melton, T.; Dong, Z.; Bowden, G. T. Stabilization of quercetin paradoxically reduces its proapoptotic effect on UVB-irradiated human keratinocytes. *Cancer Prev. Res.* **2008**, *1*, 362−368.

(16) Olson, E. R.; Melton, T.; Dickinson, S. E.; Dong, Z.; Alberts, D. S.; Bowden, G. T. Quercetin potentiates UVB-Induced c-Fos expression: implications for its use as a chemopreventive agent. *Cancer Prev. Res.* **2010**, *3*, 876−884.

(17) Dihal, A. A.; Tilburgs, C.; van Erk, M. J.; Rietjens, I. M.; Woutersen, R. A.; Stierum, R. H. Pathway and single gene analyses of inhibited Caco-2 differentiation by ascorbate-stabilized quercetin suggest enhancement of cellular processes associated with development of colon cancer. *Mol. Nutr. Food Res.* **2007**, *51*, 1031−1045.

(18) Boulton, D. W.; Walle, U. K.; Walle, T. Fate of the flavonoid quercetin in human cell lines: Chemical instability and metabolism. *J. Pharm. Pharmacol.* **1999**, *51*, 353−359.

(19) Zenkevich, I. G.; Eshchenko, A. Y.; Makarova, S. V.; Vitenberg, A. G.; Dobryakov, Y. G.; Utsal, V. A. Identification of the products of oxidation of quercetin by air oxygen at ambient temperature. *Molecules* **2007**, *12*, 654−672.

(20) Makris, D. P.; Rossiter, J. T. Heat-induced, metal-catalyzed oxidative degradation of quercetin and rutin (Quercetin 3-O-rhamnosylglucoside) in aqueous model systems. *J. Agric. Food Chem.* **2000**, *48*, 3830−3838.

(21) Jorgensen, L. V.; Cornett, C.; Justesen, U.; Skibsted, L. H.; Dragsted, L. O. Two-electron electrochemical oxidation of quercetin and kaempferol changes only the flavonoid C-ring. *Free Radical Res.* **1998**, *29*, 339−350.

(22) Fahlman, B. M.; Krol, E. S. UVA and UVB radiation-induced oxidation products of quercetin. *J. Photochem. Photobiol., B* **2009**, *97* (3), 123−131.

(23) Smith, G. J.; Thomsen, S. J.; Markham, K. R.; Andary, C.; Cardon, D. The photostabilities of naturally occurring 5-hydroxyflavones, flavonols, their glycosides and their aluminium complexes. *J. Photochem. Photobiol., A* **2000**, *136*, 87−91.

(24) Smith, G. J.; Markham, K. R. Tautomerism of flavonol glucosides: relevance to plant UV protection and flower colour. *J. Photochem. Photobiol., A* **1998**, *118*, 99−105.

(25) Takahama, U. O_2^--dependent and -independent photooxidation of quercetin in the presence and absence of riboflavin and effects of ascorbate on the photooxidation. *Photochem. Photobiol.* **1985**, *42*, 89−91.

(26) Kaneta, M.; Sugiyama, N. The light resistance of the flavones and the flavonols. *Bull. Chem. Soc. Jpn.* **1971**, *44*, 3211.

(27) Ferreira, E. S. B.; Quye, A.; McNab, H.; Hulme, A. N. Photo-oxidation products of quercetin and morin as markers for the characterization of natural flavonoid yellow dyes in ancient textiles. *Dyes Hist. Achaeol.* **2002**, *18*, 63−72.

(28) Kim, M. K.; Park, K. S.; Lee, C.; Park, H. R.; Choo, H.; Chong, Y. Enhanced stability and intracellular accumulation of quercetin by protection of the chemically or metabolically susceptible hydroxyl groups with a pivaloxymethyl (POM) promoiety. *J. Med. Chem.* **2010**, *53*, 8597−8607.
(29) Vicentini, F. T.; Vaz, M. M.; Fonseca, Y. M.; Bentley, M. V.; Fonseca, M. J. Characterization and stability study of a water-in-oil microemulsion incorporating quercetin. *Drug Dev. Ind. Pharm.* **2011**, *37*, 47−55.
(30) Fang, R.; Hao, R.; Wu, X.; Li, Q.; Leng, X.; Jing, H. Bovine serum albumin nanoparticle promotes the stability of quercetin in simulated intestinal fluid. *J. Agric. Food Chem.* **2011**, *59*, 6292−6298.
(31) Scalia, S.; Mezzena, M. Incorporation of quercetin in lipid microparticles: effect on photo- and chemical-stability. *J. Pharm. Biomed. Anal.* **2009**, *49*, 90−94.
(32) Liazid, A.; Palma, M.; Brigui, J.; Barroso, C. G. Investigation on phenolic compounds stability during microwave-assisted extraction. *J. Chromatogr., A* **2007**, *1140*, 29−34.
(33) Krishnamachari, V.; Levine, L. H.; Zhou, C.; Pare, P. W. In vitro flavon-3-ol oxidation mediated by a B ring hydroxylation pattern. *Chem. Res. Toxicol.* **2004**, *17*, 795−804.
(34) Biesaga, M. Influence of extraction methods on stability of flavonoids. *J. Chromatogr., A* **2011**, *1218*, 2505−2512.
(35) Krishnamachari, V.; Levine, L. H.; Pare, P. W. Flavonoid oxidation by the radical generator AIBN: a unified mechanism for quercetin radical scavenging. *J. Agric. Food Chem.* **2002**, *50*, 4357−4363.
(36) Weinert, E. E.; Dondi, R.; Colloredo-Melz, S.; Frankenfield, K. N.; Mitchell, C. H.; Freccero, M.; Rokita, S. E. Substituents on quinone methides strongly modulate formation and stability of their nucleophilic adducts. *J. Am. Chem. Soc.* **2006**, *128*, 11940−11947.
(37) de Souza, R. F. V.; Sussuchi, E. M.; De Giovani, W. F. Synthesis, electrochemical, spectral, and antioxidant properties of complexes of flavonoids with metal ions. *Synth. React. Inorg. Met. Org. Chem.* **2003**, *33*, 1125−1144.
(38) Long, L. H.; Clement, M. V.; Halliwell, B. Artifacts in cell culture: rapid generation of hydrogen peroxide on addition of (−)-epigallocatechin, (−)-epigallocatechin gallate, (+)-catechin, and quercetin to commonly used cell culture media. *Biochem. Biophys. Res. Commun.* **2000**, *273*, 50−53.
(39) Bellion, P.; Olk, M.; Will, F.; Dietrich, H.; Baum, M.; Eisenbrand, G.; Janzowski, C. Formation of hydrogen peroxide in cell culture media by apple polyphenols and its effect on antioxidant biomarkers in the colon cell line HT-29. *Mol. Nutr. Food Res.* **2009**, *53*, 1226−1236.
(40) Sim, G. S.; Lee, B. C.; Cho, H. S.; Lee, J. W.; Kim, J. H.; Lee, D. H.; Kim, J. H.; Pyo, H. B.; Moon, D. C.; Oh, K. W.; Yun, Y. P.; Hong, J. T. Structure activity relationship of antioxidative property of flavonoids and inhibitory effect on matrix metalloproteinase activity in UVA-irradiated human dermal fibroblast. *Arch. Pharm. Res.* **2007**, *30*, 290−298.
(41) Park, S. S.; Bae, I.; Lee, Y. J. Flavonoids-induced accumulation of hypoxia-inducible factor (HIF)-1alpha/2alpha is mediated through chelation of iron. *J. Cell Biochem.* **2008**, *103*, 1989−1998.
(42) Szliszka, E.; Czuba, Z. P.; Domino, M.; Mazur, B.; Zydowicz, G.; Krol, W. Ethanolic extract of propolis (EEP) enhances the apoptosis-inducing potential of TRAIL in cancer cells. *Molecules* **2009**, *14*, 738−754.
(43) Tolomeo, M.; Grimaudo, S.; Di Cristina, A.; Pipitone, R. M.; Dusonchet, L.; Meli, M.; Crosta, L.; Gebbia, N.; Invidiata, F. P.; Titone, L.; Simoni, D. Galangin increases the cytotoxic activity of imatinib mesylate in imatinib-sensitive and imatinib-resistant Bcr-Abl expressing leukemia cells. *Cancer Lett.* **2008**, *265*, 289−297.
(44) Monasterio, A.; Urdaci, M. C.; Pinchuk, I. V.; Lopez-Moratalla, N.; Martinez-Irujo, J. J. Flavonoids induce apoptosis in human leukemia U937 cells through caspase- and caspase-calpain-dependent pathways. *Nutr. Cancer* **2004**, *50*, 90−100.
(45) Murray, T. J.; Yang, X.; Sherr, D. H. Growth of a human mammary tumor cell line is blocked by galangin, a naturally occurring bioflavonoid, and is accompanied by down-regulation of cyclins D3, E, and A. *Breast Cancer Res.* **2006**, *8*, R17.
(46) Raso, G. M.; Meli, R.; Di Carlo, G.; Pacilio, M.; Di Carlo, R. Inhibition of inducible nitric oxide synthase and cyclooxygenase-2 expression by flavonoids in macrophage J774A.1. *Life Sci.* **2001**, *68*, 921−931.